Ex-situ XPS study of the interface between a Ag(111) electrode and an alkaline electrolyte. 1. Influence of the emersion potential on the adsorption of oxygen species

Ex Situ X-ray Photoelectron Spectroscopy Study of the Interface between a Ag(111) Electrode and an Alkaline Electrolyte. 1. Influence of the Electrode Potential on the Adsorption of Oxygen Species

E. R. Savinova,*,‡ D. Zemlyanov,‡ A. Scheybal,† Th. Schedel-Niedrig,† K. Doblhofer,† and R. Schlögl†

Fritz-Haber-Institut der Max-Planck-Gesellschaft, Faradayweg 4-6, D-14195 Berlin, Germany, and Boreskov Institute of Catalysis, Russian Academy of Sciences, Pr. Akademika Lavrentieva 5, 630090 Novosibirsk, Russian Federation

Received December 30, 1998. In Final Form: April 7, 1999

A Ag(111) single-crystal electrode emersed from the NaF + NaOH electrolyte (pH 11) under the anodic polarization has been studied ex situ by means of X-ray photoelectron spectroscopy. The oxidation of the electrode starts at −0.6 V vs Hg/HgO (ca. 1 V negative to the reversible potential of Ag_2O phase formation) and manifests itself by the appearance of different surface and bulk oxygen-containing species. These are surface OH groups (OH_{ads}), surface oxide-like species ($O_{ads}^{\delta-}$), and bulk OH groups (OH_{bulk}). The OH_{bulk} exhibit high thermal stability in a vacuum but can be efficiently removed from the electrode via cathodic polarization.

1. Introduction

The adsorption of oxygen species on a metal/electrolyte interface plays an important role in electrocatalysis. Thus, it is usually accepted that oxidation of organic molecules on Pt and other metal electrodes involves the adsorbed hydroxide species.[1] This has been recently proven for Pt−Ru nanoparticles[2,3] by means of X-ray absorption near-edge structure and extended X-ray absorption fine structure and for polycrystalline Ni and Fe[4] by potential-modulated reflectance spectroscopy.

Electrochemical reduction of oxygen, hydrogen peroxide on Pt,[5] Ru,[6] Ag,[7−10] Au,[11,12] and Cu[13,14] and peroxodisulfate on Cu[15] electrodes proceeds apparently through the formation of strongly bound oxygen-containing adsorbates, in particular, adsorbed hydroxide groups. Various oxygen species on the surface and in the subsurface may influence the above-mentioned reactions both as catalysts as well as inhibitors.

Silver attracts much attention because of its catalytic activity in a number of important chemical and electrochemical processes. It is a unique metal catalyst for ethylene epoxidation[16,17] and a catalyst for methanol oxidation and other organic reactions.[18,19] Silver is also of considerable importance as an electrode material for battery and fuel cell applications, in particular, due to its electrocatalytic activity in the electroreduction of oxygen and hydrogen peroxide.[7−9,20,21] Despite the practical importance of the above-mentioned reactions, their mechanisms on a silver electrode are still not clear. It has been postulated that the electrocatalytic properties of silver depend crucially on the formation of particular oxygen/hydroxide adsorbates in the potential region below Ag_2O formation.[9,10] Formation of electrochemisorbed hydroxide (OH_{ads}) and oxide species on a Ag(111) electrode in alkaline NaF/NaOH electrolytes in the potential range of the hydrogen peroxide reduction (between −1.0 and 0.2 V vs Hg/HgO, depending on pH) has been proven by means of in situ surface-enhanced Raman scattering (SERS).[22] OH_{ads} species have been observed also on the electrochemical interface between polycrystalline Ag(pc) and NaOH.[23]

A large body of research performed during the last 20 years has shown that ex situ studies of the emersed

* To whom correspondence should be addressed. Fax: +7 3832 34 30 56. E-mail: elensav@catalysis.nsk.su.

† Fritz-Haber-Institut der Max-Planck-Gesellschaft.

‡ Russian Academy of Sciences.

(1) Parsons, R.; VanderNoot, T. *J. Electroanal. Chem.* **1988**, *9*, 257.
(2) Aberdam, D.; Durand, R.; Faure, R.; Gloaguen, F.; Hazemann, J. L.; Herrero, E.; Kabbabi, A.; Ulrich, O. *J. Electroanal. Chem.* **1995**, *398*, 43.
(3) McBreen, J.; Mukerjee, S. *J. Electrochem. Soc.* **1995**, *142*, 3399.
(4) Kowal, A.; Gutierrez, C. *J. Electroanal. Chem.* **1995**, *395*, 243.
(5) Burke, L. D.; Casey, J. K. *Ber. Bunsen-Ges. Phys. Chem.* **1990**, *94*, 931.
(6) Nekrasov, L. I.; Khrusheva, E. I. *Elektrokhimiya* **1967**, *3*, 166 (in Russian).
(7) Brezina, M.; Koryta, J.; Musilova, M. *Collect. Czechoslov. Chem. Commun.* **1968**, *33*, 3397.
(8) Honda, M.; Kodera, T.; Kita, H. *Electrochim. Acta* **1983**, *28*, 727.
(9) Honda, M.; Kodera, T.; Kita, H. *Electrochim. Acta* **1986**, *31*, 377.
(10) Savinova, E. R.; Wasle, S.; Doblhofer, K. *Electrochim. Acta* **1998**, *44*, 1341.
(11) Strbac, S.; Adzic, R. R. *J. Electroanal. Chem.* **1996**, *403*, 169.
(12) Burke, L. D.; Lee, B. H. *J. Electroanal. Chem.* **1992**, *330*, 637.
(13) Vasquez, M. V.; de Sanchez, S. R.; Calvo, E. J.; Schiffrin, D. J. *J. Electroanal. Chem.* **1994**, *374*, 179.
(14) King, F.; Quinn, M. J.; Litke, C. D. *J. Electroanal. Chem.* **1995**, *385*, 45.
(15) Härtinger, S.; Rosenmund, J.; Savinova, E. R.; Wasle, S.; Doblhofer, K. *J. Phys. Chem. B* **1997**, *101*, 2411.
(16) Barteau, M. A.; Madix, R. J. In *The Chemical Physics of Solid Surface and Heterogeneous Catalysis: Fundamental Studies of Heterogeneous Catalysis*; King, D. A., Woodruff, D. P., Eds.; Elsevier: Amsterdam, 1982; Vol. 4, p 95.
(17) Gland, R. B.; Lambert, R. M. *J. Catal.* **1985**, *92*, 364.
(18) Bao, X.; Muhler, M.; Pettinger, B.; Schlögl, R.; Ertl, G. *Catal. Lett.* **1993**, *22*, 215.
(19) Herein, D.; Nagy, A.; Schubert, H.; Weinberg, G.; Kitzelmann, E.; Schlögl, R. *Z. Phys. Chem.* **1996**, *197*, 67.
(20) Brezina, M.; Koryta, J.; Phuong, P.-T. L. *J. Electroanal. Chem.* **1972**, *40*, 107.
(21) Kicheev, A. G.; Sheblovinskii, V. M. *Electrokhimiya* **1983**, *19*, 1071 (in Russian).
(22) Savinova, E. R.; Kraft, P.; Pettinger, B.; Doblhofer, K. *J. Electroanal. Chem.* **1997**, *430*, 47.
(23) Iwasaki, N.; Sasaki, Y.; Nishina, Y. *Surf. Sci.* **1988**, *198*, 524.

10.1021/la9817617 CCC: $18.00
Published on Web 07/23/1999

electrodes in an ultrahigh vacuum (UHV) using surface physics techniques can provide valuable information on the structure and composition of an electrode/electrolyte interface (see, e.g., refs. 24−34[24–34] and references therein). Recently, ex situ X-ray photoelectron spectroscopy (XPS) has proven to be an effective means for studying oxygen species formed on the interface between Ag(pc) and NaCl/NaOH,[35] NaBr/NaOH[36] solutions and Ag(111), and NaF/NaOH solution[37] under anodic polarization. Thus, incorporation of OH species in the bulk of the electrode under mild anodic polarization (0.0 and +0.2 V vs Hg/HgO at pH 11) has been for the first time observed by ex situ XPS.[37] The objective of the present work is to evaluate the effect of potential on the formation of surface and bulk oxygen species on the interface between the Ag(111) electrode and alkaline electrolyte ex situ by XPS. Part 1 is devoted to studying oxygen-containing adsorbates depending on the emersion potential, while the adsorption of sodium on the Ag(111) electrode and a tentative model of the interfacial region are considered in Part 2.[38]

2. Experimental Section

2.1. Apparatus. The experiments were carried out in a specially designed system described in detail elsewhere.[37] The system combines a glovebox (Braun) housing an electrochemical cell (EC) connected via an UHV transfer system to an analyzer stainless steel chamber of a modified Leybold LHS 12 MCD spectrometer. The advantage of this setup is a possibility to perform experiments in a conventional electrochemical cell under steady-state operation. The analyzer chamber (pressure $< 6 \times 10^{-11}$ mbar) was equipped with tools for ultraviolet photoelectron spectroscopy (UPS), XPS, and ion-scattering spectroscopy (ISS).

The XPS spectra were obtained using the Mg Kα radiation ($h\nu$ = 1253.6 eV) and a fixed analyzer pass energy of 48 eV, corresponding to a resolution of 0.9 eV measured as a full width at half-maximum (fwhm) of the Ag $3d_{5/2}$ peak. The photoelectrons were collected by a hemispherical 180° analyzer in the normal direction with respect to the surface. The binding energy (BE) values referred to the Fermi level were calibrated using the Au $4f_{7/2}$ = 84.0 eV and Cu $2p_{3/2}$ = 932.7 eV peaks. (The Ag $3d_{5/2}$ peak was set at 368.3 eV of BE.) The concentrations of the chemical elements in the near-surface region (in at. %) were estimated after the subtraction of a Shirley-type background, taking into account the corresponding atomic sensitivity factors.[39] Surface concentrations of oxygen species (N(O)) have been estimated by measuring the areas (S) of the O 1s and Ag $3d_{5/2}$ peaks and using the equation from ref 40[40] without taking into account any shielding effect:

$$N(\mathrm{O}) = (2.2 \times 10^{16}) \frac{S(\mathrm{O\ 1s})}{S(\mathrm{Ag\ 3d_{5/2}})}\ \mathrm{atoms \cdot cm^{-2}} \qquad (1)$$

Coverage was measured in monolayers (ML) in respect to the number of silver atoms in the topmost layer of the Ag(111) surface, which equals 1.38×10^{15} atoms·cm^{-2}.[41]

2.2. Electrode Preparation and Electrochemical Experiment. The single crystal used in the experiments was cut from a silver rod (Mateck, 99.999%) in the (111) direction and polished with diamond paste down to 1 μm. According to Laue X-ray diffraction measurements, the misorientation of the single crystal ranged from 0.5 to 1°. The sample cleaning was performed before each experiment and consisted of (i) reduction of the crystal in EC at −1.5 V for 10 min and (ii) conventional UHV procedures, including cycles of Ar^+ and He^+ etching and annealing in oxygen and a vacuum. A He^+ beam with a kinetic energy of 1000 eV was used for mild sputtering. The impacting He^+ current was about 1 μA. An Ar^+ beam with a kinetic energy of 2000 eV was used for severe sputtering. The impacting Ar^+ current was about 10 μA at an argon pressure of 5×10^{-8} bar. The cleanliness of the sample was controlled by means of XPS and UPS. Scanning tunneling microscopy proved that the procedures used for the sample cleaning did not damage the (111) lattice of the crystal surface.

After the completion of cleaning procedures in an UHV the sample was transferred into the glovebox filled with Ar and immersed into 5×10^{-4} M NaF + 10^{-3} M NaOH aqueous electrolyte (pH 11) under a specified potential for 10 min. Then the electrode was emersed from the electrolyte under controlled potential and transmitted under UHV conditions into the analyzer chamber. In our previous work it was shown that when the concentration of the supporting electrolyte was an order of magnitude higher, Na^+ and F^- ions from the dried up salts were observed on the Ag(111) electrode emersed under the anodic polarization. Deposition of the electrolyte hindered the analysis of the species adsorbed on the surface.[37] Since F^- is known to adsorb very slightly on Ag electrodes,[42] the presence of both NaF and NaOH in the solution allowed to the distinction between the adsorption of ions and the deposition of the electrolyte.

The validity of the emersion procedure and sample transfer was established elsewhere.[37] The sample transfer from the EC to the analyzer chamber was accompanied by an accumulation of some carbon impurities on the Ag(111) surface. The typical carbon level in the present work was below 13 at. %. The C 1s core level spectra taken from the electrode emersed under various potentials mainly show the peak at 284.5 eV, characteristic for hydrocarbons.[43] The amount of carbonates and oxygen-containing organic compounds was found to be negligible.[37] The intensity of the C 1s core level spectra of a Ag(111) electrode did not correlate with the emersion potential, and thus, organic impurities could not hinder the analysis of the oxygen species adsorption.

The Ag(111) electrode (surface area 0.87 cm^2) was electrochemically treated in a three-electrode three-compartment glass cell under an Ar atmosphere at room temperature using conventional electrochemical equipment. Platinum and Hg/HgO/0.5 M NaOH (E = 0.125 V vs NHE) were used as a counter and reference electrode, respectively. All the electrode potentials quoted are relative to the Hg/HgO electrode. The reference electrode was connected to the cell via a Luggin capillary.

Solutions of NaOH and NaF were freshly prepared from NaOH·H_2O (suprapure Merck), NaF (suprapure Merck), and triply distilled water in the glovebox under an Ar atmosphere. Triply distilled water was boiled under an Ar atmosphere to remove CO_2 and oxygen.

3. Results and Discussion

3.1. Electrochemical characterization of the Ag(111)/Electrolyte Interface. Figure 1 shows a cyclic

(24) Ansell, R. O.; Dickinson, T.; Povey, A. F.; Sherwood, P. M. A. *J Electroanal. Chem.* **1979**, *98*, 69.
(25) Sherwood, P. M. A. *Chem. Soc. Rev.* **1985**, *14*, 1.
(26) Hansen, W. N. *J. Electroanal. Chem.* **1983**, *150*. 133.
(27) D'Agostino, A. T.; Hansen, W. N. *Surf. Sci.* **1986**, *165*, 268.
(28) Kolb, D. M.; Rath, D. L.; Wille, R.; Hansen, W. N. *Ber. Bunsen-Ges. Phys. Chem.* **1983**, *87*, 1108.
(29) Neff, H.; Kötz, R. J. *Electroanal. Chem.* **1983**, *151*, 305.
(30) Kötz, E. R.; Neff, H.; Müller, K. J. *Electroanal. Chem.* **1986**, *215*, 331.
(31) Wagner, F. T. In *Structure of Electrified Interfaces*; Lipkowski, J., Ross, P. N., Eds.; VCH Publishers: New York, 1993.
(32) Hubbard, A. T. *Chem. Rev.* **1988**, *88*, 633.
(33) Haupt, S.; Collisi, U.; Speckmann, H. D.; Strehblow, H.-H. *J. Electroanal. Chem.* **1985**, *194*, 179.
(34) Stuve, E. M.; Krasnopoler, A.; Sauer, D. E. *Surf. Sci.* **1995**, *335*, 177.
(35) Hecht, D.; Strehblow, H.-H. *J. Electroanal. Chem.* **1997**, *440*, 211.
(36) Luetzenkirchen-Hecht, D.; Strehblow, H.-H. *Ber. Bunsen-Ges. Phys. Chem.* **1998**, *102*, 826.
(37) Zemlyanov, D. Y.; Savinova, E. R.; Scheybal, A.; Doblhofer, K.; Schlögl, R. *Surf. Sci.* **1998**, *418*, 441.
(38) Savinova, E. R.; Zemlyanov, D. Y.; Scheybal, A.; Doblhofer, K.; Schlögl, R. *Langmuir* **1999**, *15*, 6552.
(39) Yeh, J. J.; Lindau, I. *At. Data Nucl. Data Tables* **1985**, *32*, 1.
(40) Bukhtiyarov, V. I.; Boronin, A. I.; Savchenko, V. I. *J. Catal.* **1990**, *150*, 262.
(41) Bare, S. R.; Griffiths, K.; Lennard, W. N.; Tang, H. T. *Surf. Sci.* **1995**, *342*, 185.
(42) Valette, G.; Hamelin, A. *Electroanal. Chem. Interfacial Electrochem.* **1973**, *45*, 301.
(43) Weaver, J. F.; Hoflund, G. B. *J. Phys. Chem.* **1994**, *98*, 8519 and references therein.

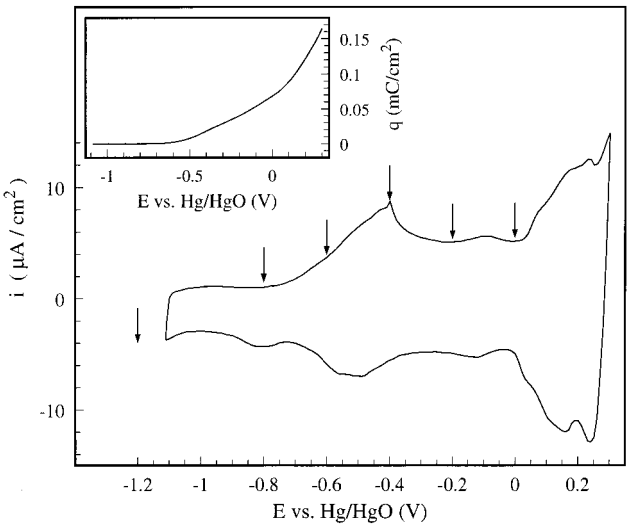

Figure 1. Cyclic voltammogram of the Ag(111) electrode in 5 × 10^{-4} M NaF + 10^{-3} M NaOH. Sweep rate is 0.05 V s^{-1}. The arrows indicate the potentials where the XPS analysis was performed. The inset shows the charge transferred in the anodic sweep of the voltammogram.

voltammogram of the Ag(111) electrode cleaned in the UHV chamber and immersed into the 5 × 10^{-4} M NaF + 10^{-3} M NaOH electrolyte solution without contact with the atmosphere. The obtained voltammogram corresponds well to the one presented in ref 44[44] for 0.1 M NaOH solution, but is shifted by ca. 0.1 V in the positive direction. The increase of the cathodic current at potentials as negative as −1.1 V is caused by the onset of the hydrogen evolution reaction. A steep increase of the current at potentials above 0.3 V can be attributed to the anodic silver oxidation ($E_{Ag_2O/Ag} = 0.342 - RT/F \ln[OH^-]$, V vs NHE[45]). According to our previous studies, the anodic and cathodic maxima observed in the potential interval between hydrogen evolution and bulk silver oxidation are pH-dependent and concerned with hydroxide electrochemisorption.[10,22] The shapes of the anodic and cathodic peaks point to the complex multistep mechanism of the chemisorption process. The chemisorption charge was calculated from the voltammogram after subtraction of the charging current (that was assumed to have the same value as measured at E below −0.8 V) and is represented in the inset of Figure 1.

3.2. XPS Characterization of an Ag(111) Electrode Emersed under Various Potentials. Figure 2 represents the O 1s core level spectra obtained from the Ag(111) electrode emersed from the electrolyte under various potentials. The intensity of the O 1s peak from the electrode emersed at a potential equal to or below −0.8 V does not differ significantly from the spectrum of the clean sample. Anodic polarization of the electrode from −0.8 V to the potential region of the voltammetric peaks shown in Figure 1 results in increasing the overall intensity of the O 1s peaks along with an alteration of their shapes. This unambiguously points to the formation of a number of oxygen species with different BEs upon anodic polarization. From Figures 1 and 2 it is clearly visible that the appearance of the oxygen-containing adsorbates on the emersed electrode corresponds to the onset of the anodic current on the positive-going scan of the voltammogram. Contribution of a number of states to the O 1s peak makes

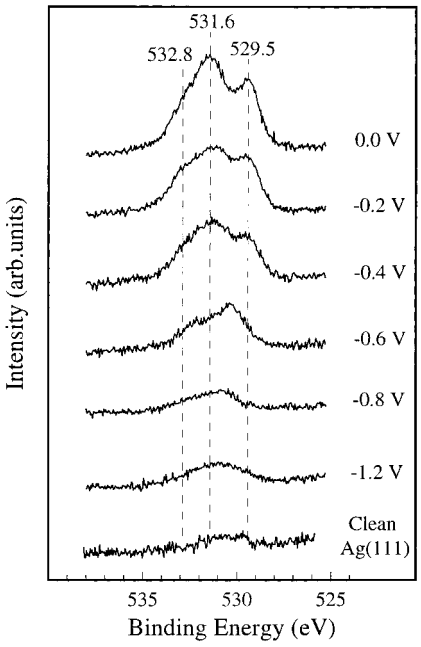

Figure 2. O 1s XP spectra taken from the Ag(111) electrode emersed from 5 × 10^{-4} M NaF + 10^{-3} M NaOH at specified potentials. The spectra were recorded at 300 K.

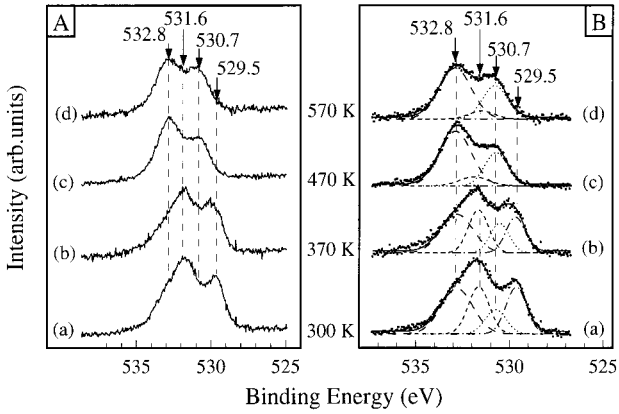

Figure 3. O 1s XP spectra taken from the Ag(111) electrode exposed at 0.0 V in 5 × 10^{-4} M NaF + 10^{-3} M NaOH for 10 min (a) and subsequently heated at 370 K (b), 470 K (c), and 570 K (d). The spectra were registered at specified temperatures. The results of the curve fit analysis are presented in the right panel.

their assignments rather sophisticated. However, since different oxygen species are characterized by remarkably different desorption temperatures (see ref 37 and references therein), the assignment of O 1s peaks prove to be feasible by means of studying their thermal stabilities.[37]

3.2.1. Assignment of Adsorbed Oxygen Species. The O 1s spectra taken after the emersion of the Ag(111) crystal from the electrolyte at 0.0 V and heating in a vacuum in a stepwise manner are represented in Figure 3. The O 1s line taken from the emersed electrode shows two well-resolved peaks at ca. 529.5 and 531.6 eV and a shoulder at 532.8 eV (Figure 3a). As expected, heating in a vacuum causes significant changes of the shape of the O 1s line. Thus, after being heated at 470 K, the peaks at 529.5 and 531.6 eV disappear, and two peaks at 530.7 and 532.8 eV become the main features of the O 1s spectrum (Figure 3c). Subsequent heating at 570 K slightly changes only the ratio between these peaks but does not alter their intensities significantly.

(44) Stevenson, K. J.; Gao, X.; Hatchett, D. W.; White, H. S. *J. Electroanal. Chem.* **1998**, *447*, 43.

(45) *CRC Handbook of Chemistry and Physics*; Weast, R. C., Astle, M. J., Eds.; CRC Press: Boca Raton, FL, 1982.

Table 1. O 1s BE and Properties of the Oxygen Species Formed on the Ag(111) Electrode under Anodic Polarization

assignment	O 1s BE, eV	localization	thermal stability
$O_{ads}^{\delta-}$	529.5 ± 0.2	surface	decomposes below 470 K
OH_{ads}	531.6 ± 0.1	surface	desorbs at 470 K
OH_{bulk}	532.8 ± 0.1	bulk	stable up to 750 K
O_β	530.7 ± 0.1	bulk	depends on conditions[a]

[a] See discussion elsewhere.[37]

The curve fit analysis based on these findings allows one to distinguish four components of the O 1s state at 529.5 ± 0.2, 530.7 ± 0.1, 531.6 ± 0.1, and 532.8 ± 0.1 eV, as shown in the right panel of Figure 3. The curve fit analysis was performed after subtraction of a Shirley-type background, assuming a Gaussian shape of lines. A comparison of the experimental results discussed above with the literature data on the different oxygen-containing species on a silver surface leads to the following assignments of the observed peaks. The less thermostable species are the OH groups adsorbed on the surface (OH_{ads}) and surface oxygen of the Ag_2O oxide-type ($O_{ads}^{\delta-}$) characterized by the peaks at 531.6 and 529.5 eV, respectively. This is in agreement with the conclusions of ref 35, where the formation of the above-mentioned species was observed on the interface between polycrystalline Ag and alkaline NaCl solutions. The peaks at 532.8 and 530.7 eV observed above 470 K are attributed to the OH groups (OH_{bulk}) and oxygen (O_β) dissolved in the bulk of the Ag(111) crystal. Any substantial contribution of the hydration water in the emersed double layer to the 532.8 eV peak at elevated temperature can be ruled out because of the high thermal stability of the latter (Table 1). The peak at 530.7 eV at room temperature may result from the joint contribution of a number of oxygen species, including surface oxygen (O_α), O_β, and probably a slight impurity of carbonate species, while above 470 K, O_β is the most likely species contributing to this peak. The assignments of oxygen species formed on the Ag(111) electrode under the anodic polarization are summarized in Table 1 and discussed in detail elsewhere.[37]

3.2.2. Influence of the Emersion Potential on the Concentrations of Oxygen Species. To establish the formation of the above-discussed O-containing species depending on the emersion potential, the curve fit analysis of the O 1s spectra shown in Figure 2 was performed, as represented in Figure 4. The atomic concentrations of these species in the near-surface region as a function of the emersion potential were estimated using the results of the curve fit analysis and are shown in Figure 5. One can see that the electrode emersed at potentials below −0.8 V is practically free of oxygen-containing adsorbates. The adsorption of oxygen species starts at −0.6 V and manifests itself by the appearance of the peaks centered at 529.5, 530.7, 531.6, and 532.8 eV. The atomic concentrations of OH_{ads}, $O_{ads}^{\delta-}$, and OH_{bulk} increase with an increase of the anodic polarization (Figure 5). The coverage of the Ag(111) electrode emersed at 0.0 V with OH_{ads}, $O_{ads}^{\delta-}$, and OH_{bulk} species, estimated using eq 1, was equal to ca. 0.15, 0.15, and 0.3 ML, respectively. The absence of any correlation of the intensity of the O 1s peak at 530.7 eV with the electrode potential is apparently due to the contribution of a number of species such as O_α, O_β, and probably carbonate species to this peak at room temperature.

To evaluate the onset potential of the formation of the bulk O-containing species, the electrode emersed under various potentials was heated to 570 K in a vacuum. Figure 6 represents a set of the O 1s core level spectra taken from the Ag(111) electrode emersed from the electrolyte at the specified potentials and subsequently heated in a vacuum at 570 K. The detailed curve fit analysis of the original spectra are represented in the right panel of Figure 6. The atomic concentrations of the oxygen species vs the emersion potential are plotted in Figure 7. The most remarkable feature is that the heating results in a strong decrease of the O 1s lines from the electrode emersed below −0.4 V, so that only a weak and broad feature centered at about 531.6 eV remains after heating at 570 K. For the emersion potential above −0.4 V, the heating does not cause a considerable decrease of the overall intensity of the O 1s line. However, a redistribution of the intensities for different oxygen states is observed, as described above for the emersion potential of 0.0 V. Thus, the peaks at

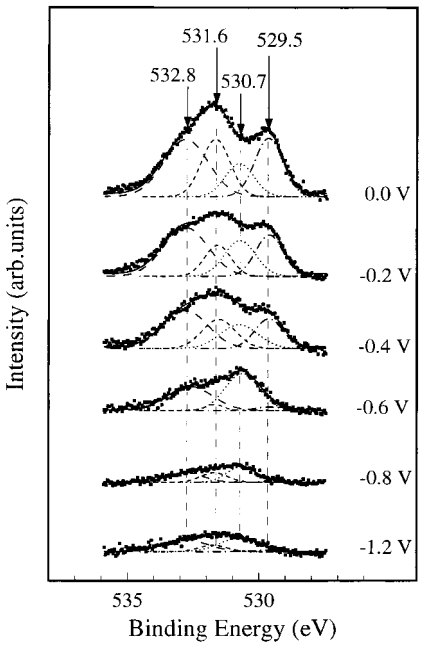

Figure 4. The curve fit analysis of the O 1s XP spectra shown in Figure 2.

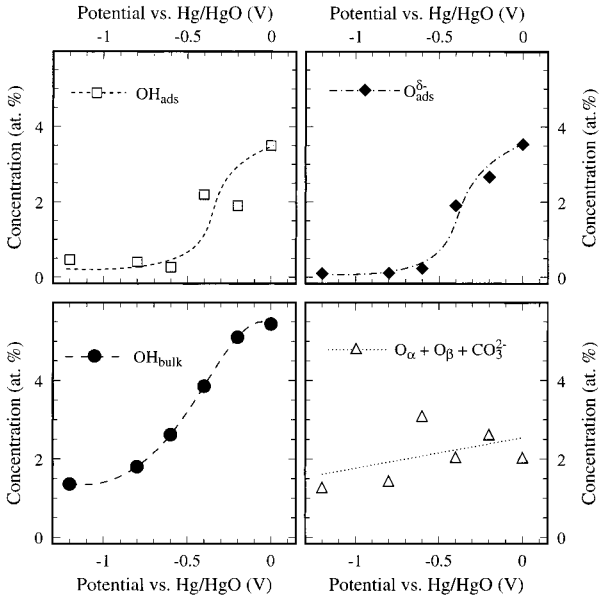

Figure 5. Effect of the emersion potential on the concentrations of oxygen-containing species on the surface of the emersed Ag(111) electrode. The concentrations were calculated on the basis of the curve fit analysis represented in Figure 4.

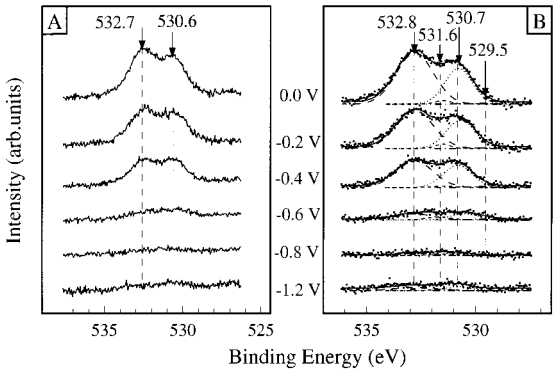

Figure 6. O 1s XP spectra taken from the Ag(111) electrode emersed at specified potentials and subsequently heated in a vacuum at 570 K. The spectra were recorded at 570 K. The results of the curve fit analysis are presented in the right panel.

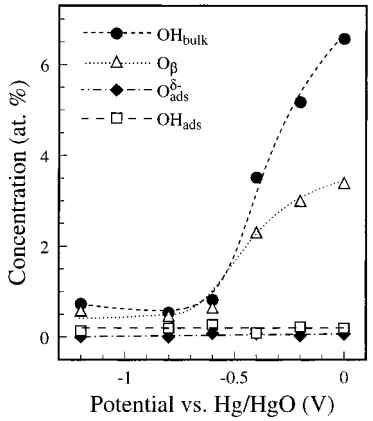

Figure 7. Effect of the potential on the concentrations of oxygen-containing species on the surface of the emersed Ag(111) electrode heated at 570 K in a vacuum. Concentrations were calculated on the basis of the curve fit analysis presented in Figure 6.

529.5 and 531.6 eV disappear after heating, reflecting the decomposition of the $O_{ads}^{\delta-}$ and OH_{ads} species. Even if the hydration water was present in the emersed double layer in UHV at room temperature and contributed to the peak at 532.8 eV, the presence of the latter after heating at 570 K strongly suggests that the OH groups incorporate in the bulk of the emersed electrode starting from −0.4 V. It is remarkable that the O 1s peak at 530.7 eV from the electrode heated to 570 K shows a distinct potential dependence (Figure 7), in contrast to the results obtained at 300 K.

3.2.3. Arguments for the Electrochemical Origin of Oxygen Species on the Emersed Electrode. It is important to clarify whether all of the oxygen species observed on the emersed electrode with the ex situ XPS are formed under electrochemical conditions or result from secondary reactions proceeding upon heating in UHV. Since the adsorption of hydroxide ions from alkaline electrolytes is supposed to be the first step of Ag electrode oxidation,[22,23] an observation of OH_{ads} on the emersed electrode was in line with our expectations. As to $O_{ads}^{\delta-}$, it is important to verify that the latter is not a product of the OH_{ads} decomposition in UHV according to reaction 2:

$$OH_{ads} + OH_{ads} + \delta e^- \leftrightarrow O_{ads}^{\delta-} + H_2O \qquad (2)$$

To check this possibility, an adsorption layer of OH_{ads} was prepared on the Ag(111) surface by the exposure of the crystal to the atmosphere of the glovebox in the presence of O_2 (20 ppm) and saturated water vapor for 10 min (XP spectra not shown here). OH_{ads} is characterized by a BE of 531.6 eV and does not decompose with the formation of $O_{ads}^{\delta-}$ in UHV at 300 K. This is in agreement with the data of Au,[46] who found that OH_{ads} desorbed from Ag(110) at 320 K. (In our case, the higher desorption temperature of OH_{ads} on Ag(111) emersed from the alkaline electrolyte is likely to be a result of the presence of sodium, which is known to increase the thermal stability of oxygen species.[47]) The stability of OH_{ads} on Ag(111) in UHV at 300 K proves that $O_{ads}^{\delta-}$ is formed under the anodic polarization and does not result from the surface reaction 2. The mild sputtering of the Ag(111) electrode at 300 K with He^+ showed the presence of the OH_{bulk} after the emersion at a potential above −0.4 V and thus demonstrated that the latter was formed in the EC and was not a product of a high-temperature transformation of, e.g., OH_{ads}.[48]

The origin of the species characterized by the peak at 530.7 eV is still ambiguous and will be clarified in the forthcoming paper.[48] The 530.7 eV peak might correspond to O_β, formed either under the electrochemical conditions or most likely as a result of the high-temperature transformation of $O_{ads}^{\delta-}$. The latter assumption is very likely in view of the absence of any correlation of the intensity of the O 1s peak at 530.8 eV with the electrode potential at room temperature. Note that Weaver and Hoflund reported the formation of bulk oxygen upon decomposition of silver oxides.[43,49]

Taking into account the discussion above, one may conclude that OH_{ads}, $O_{ads}^{\delta-}$ and OH_{bulk} are formed on the Ag(111) electrode under mild anodic polarization, and thus, the ex situ XPS provides an adequate view of the adsorption layer on the surface of the immersed electrode. A comparison of the concentrations of the oxygen species vs the potential and the charge transferred in the potential sweep experiment show their good qualitative agreement (cf. Figures 1 and 5).

3.3. Electrochemical Reduction of OH_{bulk}. The OH_{bulk} was found to be the most thermostable species among those formed upon anodic polarization. Thus, OH_{bulk} did not desorb upon heating at 570 K (Figure 3d). This is in agreement with in situ SERS data obtained by Bao et al., who reported on the high thermal stability of the OH groups dissolved in silver and observed up to 850 K.[50] Weaver et al. supposed the existence of strongly bound OH groups dissolved in silver as well.[43] Meanwhile, an electrochemical reduction was found to afford fast and effective means for stripping the OH_{bulk} species from the electrode, as demonstrated in Figure 8.

As discussed above, the surface of the Ag(111) electrode emersed at 0.0 V is covered with OH_{ads}, $O_{ads}^{\delta-}$, OH_{bulk}, and $O_\beta + O_\alpha + CO_{3,ads}$ species (Figure 8b). The immersion of that electrode to EC under cathodic polarization (−1.0 V) for 10 min results in a noticeable decrease of the overall intensity of the O 1s peak and in the appearance of a peak centered at 530.8 eV (Figure 8c). Adsorbed species characterized by this peak desorb completely after heating at 570 K, as shown in Figure 8d. One can see that the resulting weak broad feature does not differ considerably from the O 1s peak observed on the clean Ag(111) surface

(46) Au, C. T.; Singh-Boparai, S.; Roberts, M. W.; Joyner, R. J. *J. Chem. Soc., Faraday Trans.* **1983**, *79*, 1779.
(47) Marbrow, R. A.; Lambert, R. M. *Surf. Sci.* **1976**, *61*, 329.
(48) Savinova, E. R.; Zemlyanov, D.; Wild, U.; Scheybal, A.; Doblhofer, K.; Schlögl, R. In preparation.
(49) Weaver, J. F.; Hoflund, G. B. *Chem. Mater.* **1994**, *6*, 1693.
(50) Bao, X.; Muhler, M.; Pettinger, B.; Uchida, Y.; Lehmpfuhl, G.; Schlögl, R.; Ertl, G. *Catal. Lett.* **1995**, *32*, 171.

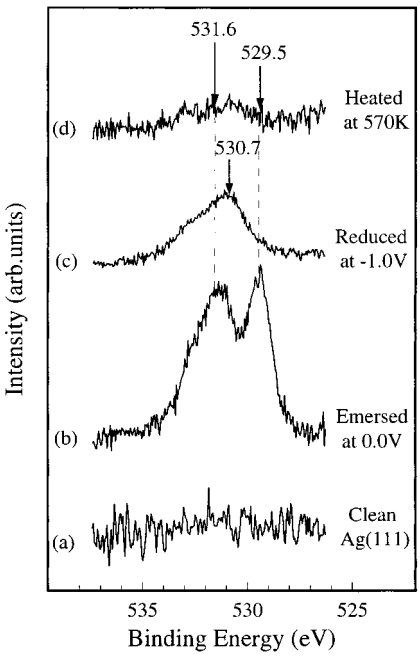

Figure 8. O 1s XP spectra obtained from the clean Ag(111) (a), from the Ag(111) electrode after the immersion in EC for 10 min at 0.0V (b), after subsequent treatment in the EC under the potential of −1.0 V for 10 min (c), and after the following heating at 570 K in UHV (d).

(Figure 8a). This strongly suggests that the bulk of the reduced electrode is practically free of the oxygen-containing species. The O 1s peaks observed on the reduced electrode at 300 K apparently correspond to some surface oxygen species and may be ascribed to OH_{ads}, O_α, and/or some impurity carbonate species. Thus, the treatment of the Ag(111) electrode at the potential negative to the current peaks observed in the cyclic voltammogram of Figure 1 results in the efficient removal of OH_{bulk} from the Ag(111) crystal. One may conclude that the electrochemical desorption of the OH_{ads} groups on the electrode surface, which proceeds under cathodic polarization of the electrode, induces the diffusion of the OH_{bulk} from the bulk of the electrode to its surface. When the fact that the surface OH_{ads} species are negatively charged is taken into account:[38] eq 3 can be formulated as

$$OH_{bulk} + e^- \rightarrow OH^-_{ads} \rightarrow OH^- \qquad (3)$$

4. Summary

As shown in the present work, XPS can be used ex situ for monitoring the effect of potential on the adsorption of oxygen species on the interface between a Ag(111) electrode and an alkaline NaF + NaOH electrolyte.

"Underpotential" oxidation of the Ag(111) electrode starts at ca. −0.6 V vs Hg/HgO (ca. 1 V negative to the reversible potential of the Ag_2O phase formation) and includes the formation of surface and bulk OH groups and surface oxide-like species. Despite the multiplicity of forms of adsorbed oxygen, their analysis proves to be feasible using gradual heating of the emersed electrode in UHV. The concentrations of surface and bulk oxygen-containing species measured by XPS increase with the anodic polarization in qualitative agreement with the data of cyclic voltammetry.

The results obtained allow one to specify the scheme of premonolayer oxidation of the Ag(111) electrode, which has been suggested earlier.[22,37] The scheme includes the adsorption of hydroxide ions from alkaline electrolyte (I), which according to Part 2[38] results in the formation of negatively charged adsorbed OH groups:

$$OH^- \rightarrow OH^-_{ads} \qquad (I)$$

The OH_{ads} under anodic polarization can be incorporated in the bulk of a Ag(111) electrode, most likely after the loss of its negative charge (II):

$$OH^-_{ads} \rightarrow OH_{bulk} + e^- \qquad (II)$$

Alternatively, the OH_{ads} can be further oxidized to give surface oxide-like species $OH^{\delta-}_{ads}$, which according to ref 38 bears a negative charge (III):

$$OH^-_{ads} + OH^- \rightarrow OH^{\delta-}_{ads} + H_2O + (2 - \delta)\, e^- \qquad (III)$$

Strongly bound OH_{bulk} species do not desorb in UHV at 570 K but can be efficiently removed from the electrode under cathodic polarization (−1.0 V vs Hg/HgO).

Acknowledgment. D.Z. gratefully acknowledges the financial support of the Alfred-Toepfer-Stiftung (Germany) and the Max-Planck-Gesellschaft in the form of a Fellowship. E.R.S. expresses her thanks to the Max-Planck-Gesellschaft for financial support. The authors would like to thank Dr. R. Schuster and Dr. X. -H. Xia for the STM measurements, Ms. S. Wasle for establishing favorable conditions for the experiments, and Ms. I. Reinhardt for proofreading the manuscript.

LA9817617